Palaeontologia Electronica
palaeo-electronica.org

Oura megale n. gen. n. sp., a large early Cambrian deuteropod with a delta-shaped tailpiece

Robert J. O'Flynn, Mark Williams, Ed Thomas, Xianguang Hou, and Yu Liu

ABSTRACT

We describe *Oura megale* n. gen. n. sp., a large (ca. 14 cm long) euarthropod from the lower Cambrian Chengjiang Konservat-Lagerstätte of Yunnan Province, China. It possesses stalked, compound eyes and a possible raptorial frontal appendage (synapomorphies and symplesiomorphies of lower stem- and upper stem-group euarthropods, respectively), but in combination with deuteropodan synapomorphies (e.g., a multi-segmented head). Micro-X-ray fluorescence shows a thorax that consists of 10 comparatively long and five comparatively short segments. The terminal segment articulates with a large, delta-shaped tailpiece that may have conferred high positional manoeuvrability in the water column. The phylogenetic position of *O. megale* n. gen. n. sp. in the euarthropod stem may add support to the homology of raptorial frontal appendages between lower stem-group euarthropods and deuteropods.

Robert J. O'Flynn. Yunnan Key Laboratory for Palaeobiology, Institute of Palaeontology, Yunnan University, 650500 Kunming, China and School of Geography, Geology and the Environment, University of Leicester, University Road, Leicester, LE1 7RH, UK and MEC International Joint Laboratory for Palaeobiology and Palaeoenvironment, Yunnan University, 650500 Kunming, China. rjof1@leicester.ac.uk
Mark Williams. School of Geography, Geology and the Environment, University of Leicester, University Road, Leicester, LE1 7RH, UK and MEC International Joint Laboratory for Palaeobiology and Palaeoenvironment, Yunnan University, 650500 Kunming, China. mri@leicester.ac.uk
Ed Thomas. School of Geography, Geology and the Environment, University of Leicester, University Road, Leicester, LE1 7RH, UK. et187@leicester.ac.uk
Xianguang Hou. Yunnan Key Laboratory for Palaeobiology, Institute of Palaeontology, Yunnan University, 650500 Kunming, China and MEC International Joint Laboratory for Palaeobiology and Palaeoenvironment, Yunnan University, 650500 Kunming, China. xghou@ynu.edu.cn
Yu Liu. Yunnan Key Laboratory for Palaeobiology, Institute of Palaeontology, Yunnan University, 650500 Kunming, China and School of Geography, Geology and the Environment, University of Leicester, University Road, Leicester, LE1 7RH, UK and MEC International Joint Laboratory for Palaeobiology and Palaeoenvironment, Yunnan University, 650500 Kunming, China. (corresponding author) yu.liu@ynu.edu.cn

https://zoobank.org/7DD733F4-6C17-4459-8213-E702764EF58B

Final citation: O'Flynn, Robert J., Williams, Mark, Thomas, Ed, Hou, Xianguang, and Liu, Yu. 2025. *Oura megale* n. gen. n. sp., a large early Cambrian deuteropod with a delta-shaped tailpiece. Palaeontologia Electronica, 28(3):a44.
https://doi.org/10.26879/1547
palaeo-electronica.org/content/2025/5687-early-cambrian-deuteropod-oura-megale

Keywords: new genus; new species; Cambrian Chengjiang biota; euarthropod; micro-X-ray fluorescence; tailpiece

Submission: 6 March 2025. Acceptance: 18 September 2025.

INTRODUCTION

Euarthropoda Lankester, 1904 is a diverse clade of segmented, jointed-limbed animals (Briggs and Parry, 2022; Vinther, 2022) with a fossil record extending to rocks of early Cambrian age, at which time they diversified rapidly (Budd, 2021) to be the most abundant group of animals in Cambrian sites of exceptional fossil preservation (Lei et al., 2024; see also Kimmig and Schiffbauer, 2024 for a modern definition of Fossil-Lagerstätten). The Chengjiang biota (ca. 518 Ma) of Yunnan Province, China is one such deposit, with exceptionally preserved fossil assemblages that provide critical morphological information bearing on the early evolution of euarthropods (e.g., Bergström and Hou, 1998; see also Hou et al., 2017 and references therein) and particularly for assessing the range of morphologies evolved by fossil deuteropods (i.e., upper stem- and crown-group euarthropods; Ortega-Hernández, 2016).

Lower stem-group euarthropods include radiodonts, exemplified by *Anomalocaris* Whiteaves, 1892, which are characterized by arthropodized frontal appendages interpreted as either protocerebral or deutocerebral (Zeng et al., 2020; see their supplementary information). Deuteropods have been, though not universally (i.e., megacheirans; see Ortega-Hernández et al., 2017, figure 3A for competing hypotheses for the alignment of head segments), defined by a differentiated deutocerebral first appendage pair [i.e., the first appendage pair (eyes are not ascribed an appendicular identity; Friedrich, 2003) is derived from the second head segment; deutocerebrum]. They have a six-segmented head, that is, a six-segmented anterior cephalic region, and exhibit dorsal arthrodization (i.e., a stiffened, articulated dorsal exoskeleton), primitively biramous limbs and arthropodization of all limbs — of which the precise evolutionary order of appearance is elusive (Ortega-Hernández, 2016). Accurate interpretations of euarthropod features potentially allow insights into the order of acquisition of characters that define fossil deuteropods, but this requires exceptionally preserved fossil evidence.

In the Chengjiang biota, non-biomineralized euarthropod soft tissues are typically replicated by pyrite (the oxidation of which gives rise to iron oxides; Lei et al., 2024) and other elements (having been buried in sediments rich in sulphate and reactive iron; Gabbott et al., 2004), and this allows their detailed anatomy to be analysed using computed tomography (CT) scanning (e.g., O'Flynn et al., 2023; Parry et al., 2024). Here we document the anatomy of *Oura megale* n. gen. n. sp., an exceptionally preserved, large deuteropod (ca. 14 cm in length), which is characterized by stalked, compound eyes, robust frontal appendages, thoracic tagmosis (the arrangement of segments into tagmata; Chipman, 2024) and a large delta-shaped tailpiece. We discuss the morphology of *O. megale* n. gen. n. sp., examine its phylogenetic relationships and evaluate the palaeoecology of this large early euarthropod, with its notably large delta-shaped tailpiece.

MATERIAL AND METHODS

Material and Measurements

Oura megale n. gen. n. sp. is known from only one specimen, recovered from the Yu'anshan Formation at Jiucun Village (24º41'33" N, 102º59'26" E), Chengjiang County, and deposited in the Yunnan Key Laboratory for Palaeobiology (YKLP). The specimen (YKLP 17237) was over-excavated by an amateur preparator, before its donation to the YKLP, which has resulted in the loss of anatomical features including parts of the head and trunk limbs. CT scanning proved unable to recover additional detail, however, the application of micro-X-ray fluorescence has recovered details of the eyes, head and trunk limbs, sternites, number of trunk and head segments and distal end of the animal. Measurements were made on digital photographs using the processing software ImageJ (Schneider et al., 2012). Overall, we have employed a combination of light photography, camera lucida drawing and micro-X-ray fluorescence to document the anatomy of *O. megale* (Figures 1–2), as described below.

Photography

The specimen was photographed (Figure 1A), in cross-polarized light (Bengtson, 2000), with a Canon EOS 5DS R fitted with a Canon EF 100 mm

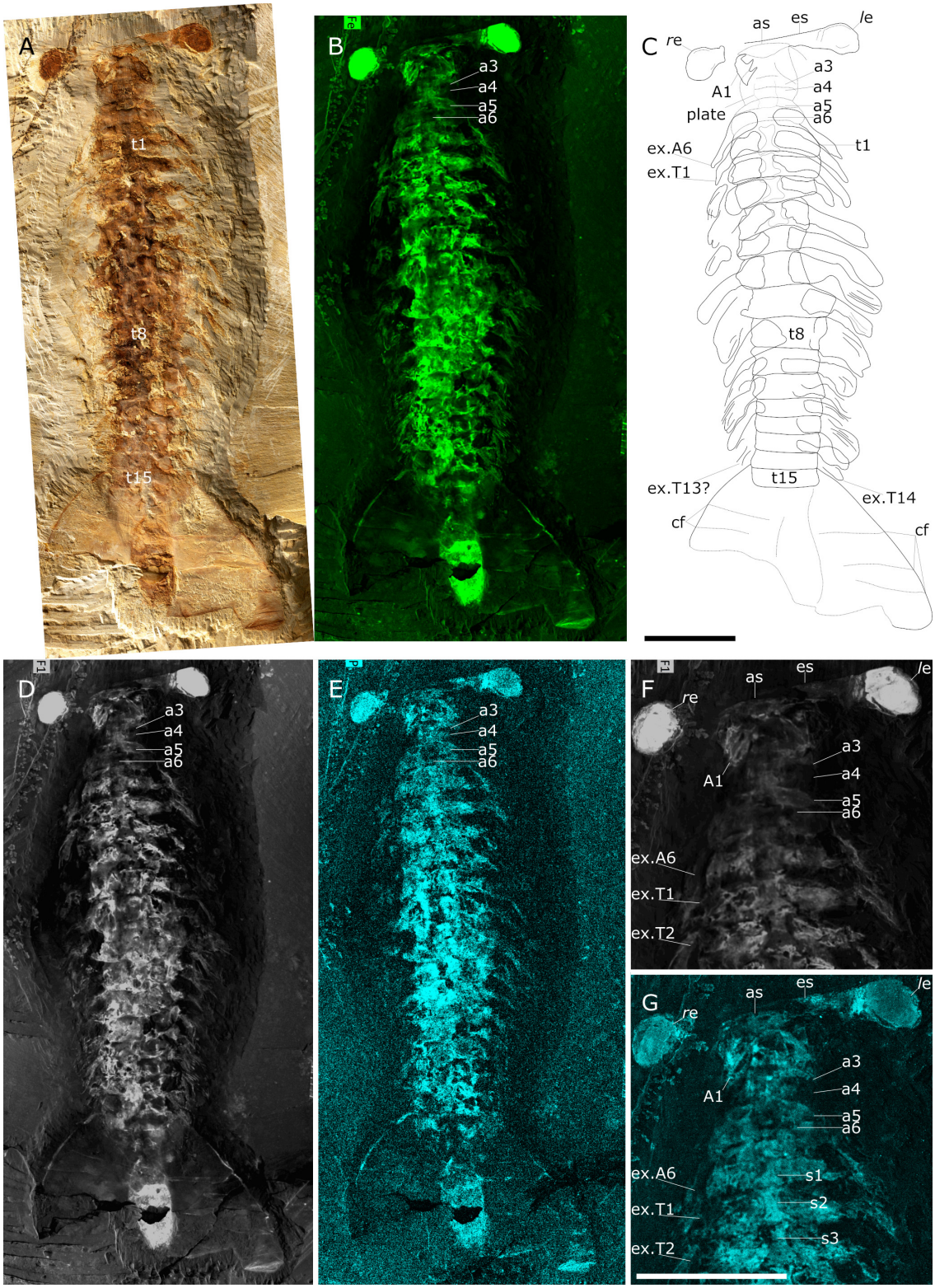

FIGURE 1. *Oura megale* n. gen n. sp. (YKLP 17237). A, photograph of ventral view. B, Fe map. C, composite line drawing. D, F1 map. E, P map. F, F1 map of head region. G, P map of head region. *Abbreviations*: *l*, left; *r*, right; A1, frontal appendage; ex.A6, exopod of 5th head limb on head segment 6; a*n*, cephalic segment (*n*); as, anterior sclerite; cf, compactional fold; e, eye; es, eye stalk; ex*n*, exopod (*n*); s*n*, sternite (*n*); T*n*, thoracic exopod (*n*); t*n*, thoracic segment (*n*). Scale bars represent 20 mm.

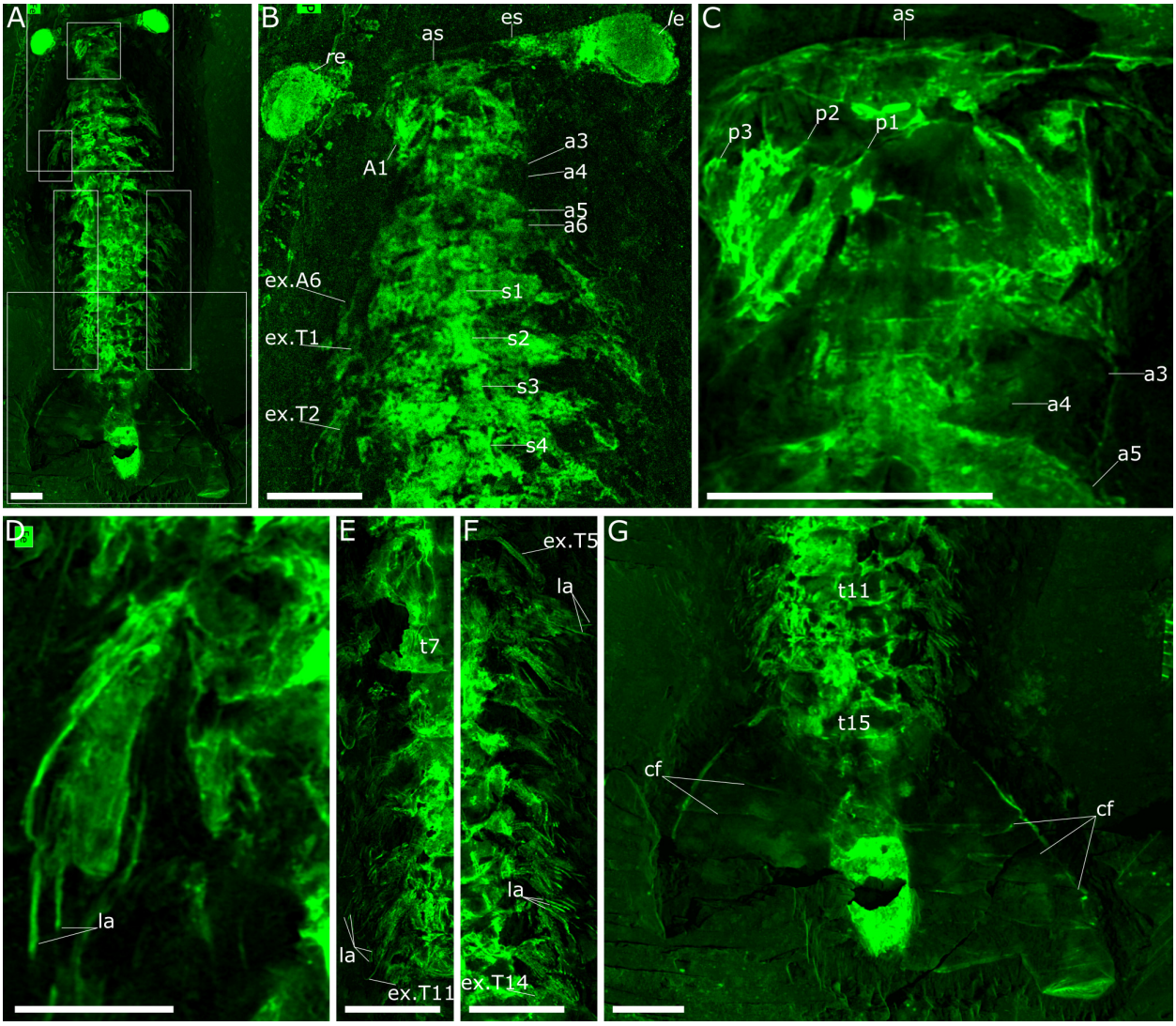

FIGURE 2. *Oura megale* n. gen n. sp. (YKLP 17237). A–G, Fe maps. B, head and anterior-most trunk region in A. C, head region in A. D, ex.T2 in A (see B for context). E–F, posterior thoracic region in A (right and left, respectively). G, posterior-most trunk region in A. *Abbreviations*: *l*, left; *r*, right; A1, frontal appendage; ex.A6, exopod of 5th head limb on head segment 6; a*n*, cephalic segment (*n*); as, anterior sclerite; cf, compactional fold; e, eye; es, eye stalk; ex*n*, exopod (*n*); la, lamella (of exopods); p*n*, podomere (*n*) (of A1); T*n*, thoracic exopod (*n*); t*n*, thoracic segment (*n*). Scale bars represent 10 mm (A–C, E–G); 5 mm (D).

F/2.8L Macro IS USM. The specimen was also investigated with computed tomography using a ZEISS Xradia 520 Versa, but no additional structures were revealed.

Micro-X-Ray Fluorescence (μXRF)

Element maps were collected using a Bruker M4 Tornado Plus (see Figure 1B, D and E for Fe, F1 and P, respectively). In addition to windowing characteristic energy ranges for specific elements, that is, the Fe Kα emission line at 6.397 ± 0.1025 keV, a free channel (F1) was designated to cover the total spectrum energy range, 25 ± 25 keV; these maps can be interpreted similarly to grey-scale backscatter electron images from scanning electron microscopy with bright areas representing higher concentrations of heavier elements. X-rays were generated using the Rh X-ray tube at an energy of 50 keV and a current of 600 mA. The X-ray beam is focused through a polycapillary lens to a spot size of approximately 20 μm and all maps used a step/pixel size of 20 μm to provide complete coverage with no pixel overlap or averaging. The chamber atmosphere was set to a vacuum of 2 mbar. These analytical conditions coupled with the light element window and dual silicon drift detec-

tors aim to optimize measuring the widest range of elements simultaneously and to keep collection times reduced.

Mapping with μXRF is non-destructive and requires no sample preparation making it an ideal technique for fossil samples. Ideally samples would be flat to reduce or eliminate any topographic effects, however, this is not the case for *Oura megale* n. gen. n. sp. Due to the concave surface resulting from the over-preparation of the specimen, analyses were undertaken using the smallest aperture (500 μm) to increase the depth of field captured when mapping, keeping as much of the specimen in focus as possible. This ensured maximum image sharpness, but necessitated longer scan times to ensure sufficient counts to the detector.

The whole specimen scan (Figures 1B, D–E, 2A) was over a total area of 150 x 75 mm with a measurement time per pixel of 11 ms (resulting in a total scan time of 2.5 days and > 18 million individual pixel spectra). The detailed scans of the head, exopod (ex3) and the posterior exopods (Figure 2C, D and E–F, respectively) are 32 x 35 mm in area with a pixel time of 25 ms, 25 x 20 mm and 50 ms, 108 x 36 mm and 25 ms, and 98 x 28 mm and 40 ms, respectively.

X-ray fluorescence maps can reveal some sub-surface elemental information (Gueriau, 2018). However, unlike monochromatic synchrotron radiation, the benchtop micro-XRF beam energy attenuates after several hundred micrometres dependent upon the sample matrix and element energy level (Beckhoff et al., 2006). These anatomical structures buried beneath a fine layer of sediment can provide powerful additional information when describing and interpreting fossil specimens.

Interpretative line drawing

A Wild Herbrugg M5 microscope, fitted with a camera lucida, was used. The resultant interpretation was combined with the fluorescent maps (particularly Fe) to produce a digital line drawing (Figure 1C).

Phylogenetic analyses

The phylogenetic position of *Oura megale* n. gen. n. sp. was inferred using the data matrix of O'Flynn et al. (2024a) (itself modified from Zeng et al., 2020) with *Lomankus edgecombei* Parry et al., 2024 and *Oestokerkus megacholix* Edgecombe et al., 2011 (see Parry et al., 2024), added. This matrix includes 283 characters and 88 taxa (Appendix 1). The matrix was constructed in WinClada 1.00.08 (Nixon, 2002), and parsimony analyses were performed with Tree analysis using New Technology (TNT) 1.5 (Goloboff and Catalano, 2016). The software was set to retain 99,999 trees in memory and perform 10,000 replications. Each analysis included a traditional search with tree bisection and reconnection, a random seed of one and 1,000 trees saved per replicate. Jackknife supports (under equal weights), and group present/contradicted (GC) frequency differences (under implied weights) of nodes on the trees were calculated by resampling 1,000 replicates of traditional search, with a change probability of 36 and 33%, respectively for the two types of nodal supports. We also used character optimization with WinClada.

Bayesian analyses used MrBayes 3.2.7 (Ronquist et al., 2012). Bayes tree search was conducted using two runs of 15,000,000 generations, sampling every 1000 generations, with four chains. The average standard deviation of split frequencies was 0.003077. Parameters and consensus trees were summarized with a burn-in fraction of 0.20.

SYSTEMATIC PALAEONTOLOGY

Phylum EUARTHROPODA Lankester, 1904
Unranked DEUTEROPODA Ortega-Hernández, 2016
Class, Order and Family incertae sedis
Genus OURA O'Flynn, Williams and Liu, new genus

zoobank.org/E3191A62-7878-4D63-A806-852927931ECB

Type Species. *Oura megale* n. gen. n. sp., by monotypy.

Etymology. Gr. *Oura*, f. tail.

Diagnosis. As for type species, by monotypy.

Remarks. *Oura* n. gen. is ascribed to Deuteropoda — as defined by a multi-segmented head and body arthrodization (Ortega-Hernández, 2016). *Oura* n. gen. bears: stalked, compound eyes, that is, a synapomorphy and symplesiomorphy of lower stem-group Euarthropoda and Deuteropoda, respectively (Ortega-Hernández, 2016, p. 11, table 4); and robust frontal appendages (FA, i.e., A1) that insert approximately one-half the length of the head behind the eye stalks and are inferred to be deutocerebral. The proximal-most three podomeres of the right-side frontal appendage (FA) are preserved, and these are morphologically like those of radiodonts and certain 'great appendage'-bearing deuteropods.

Oura megale O'Flynn, Williams and Liu, new species
Figures 1–2

zoobank.org/8A866DA3-8457-4198-B6EF-A07827904DB2

Type material. YKLP 17237 (Figure 1A) from the Cambrian, Series 2, Stage 3, *Eoredlichia–Wutingaspis* Trilobite Biozone, Yu'anshan Formation.

Etymology. Gr. *Megale*, large, great.

Diagnosis. Six cephalic segments. From anterior to posterior, these are: oblate spheroidal anterior sclerite to which large ovate paired stalked lateral eyes are attached; post-ocular segment with paired uniramous deutocerebral FAs; and four subsequent segments. FA antero-laterally orientated, consisting of ≥ three podomeres that bear elongate triangular spines. Thorax consists of 15 segments (anterior-most 10 comparatively long; posterior-most five comparatively short), each with one pair of presumed biramous appendages. Segment 15 articulated with large, ogival delta tailpiece.

Description. *Oura megale* n. gen. n. sp. is approximately 14 cm long (anterior margin of anterior sclerite to maximum posterior termination of tailpiece) and approximately 600% as-long-as it is wide (maximum width at second, third and fourth thoracic segments). It is dorsoventrally compressed, lies parallel to lamination and is well-articulated, that is, the eyes, and the thoracic sternites, the fifteenth of which articulates with a large tailpiece, are preserved in situ.

The six-segmented head is sub-rectangular, with smoothly rounded posterolateral margins, and its length, which is comparable to its width, is approximately one-seventh of the total length of the body (i.e., 20 of 140 mm). The eyes, which articulate with the oblate spheroidal anterior sclerite, are stalked and compound and extend perpendicular to the thorax. The FA inserts on the head ventrally and behind the eyes. It bears at least three podomeres (on the right side, the left being absent), each with a lateral spine that are of subequal length and width. Head segments three–six are short and narrow (Figure 2B–C), and the appendages of segment six are preserved (Figures 1C, F–G, 2B).

The thorax tapers very gently from the third to the tenth segment, after which, the eleventh segment is characterized by an abrupt change in length [4.4 mm (segment 11) versus 5.8 mm (segment 10)]. Segments 11–15 are of equivalent length and width, that is, comparatively short and narrow (4.4 mm long and 14 mm wide, respectively). Segment 15 is articulated with a very wide, ogival delta tailpiece.

The tailpiece is broad (Figure 2G; see also Figure 3 for tailpiece comparison), that is, 265% of the width of the thorax's broadest segments (i.e., first, second and third; 55 mm versus 20 mm), but the posterior margin of the middle as well as its left, cannot be described further because it is partly hidden underneath the matrix.

Fifteen pairs of exopods are observed associated with head segment six and thoracic segments t1–14, showing transverse lines, that is, they are lamellate. No appendages are observed in association with cephalic segments three–five or thoracic segment 15.

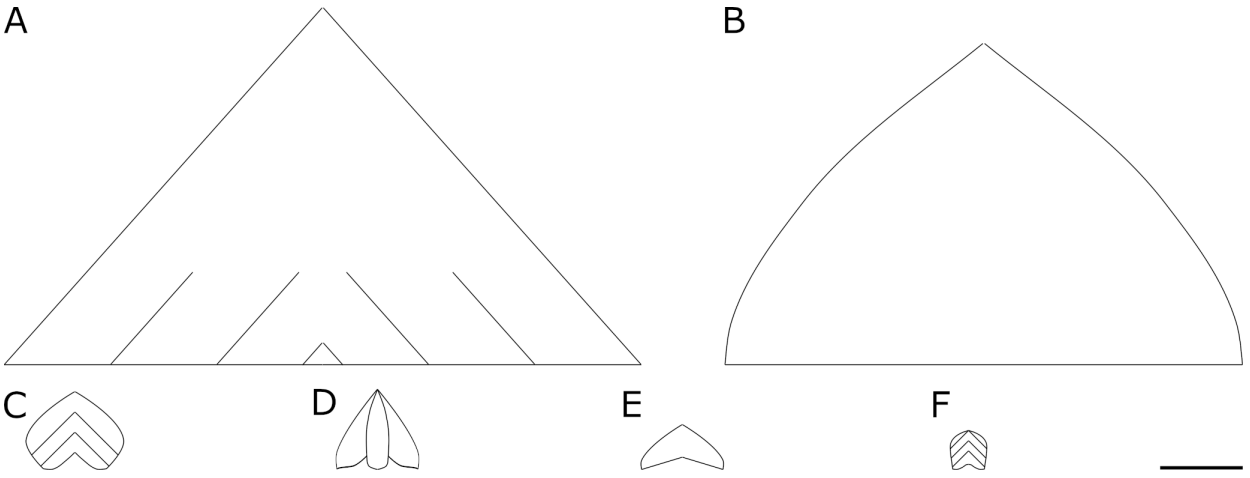

FIGURE 3. Tailpiece comparison. A, *Anomalocaris canadensis* Whiteaves 1892 based on Daley and Edgecombe (2014) and Sheppard et al. (2018). B, *Oura megale* n. gen. n. sp. C. *Opabinia* Budd, 1998 based on Legg and Vannier 2013. D, *Kylinxia zhangi* Zeng, Zhao and Huang in Zeng et al., 2020. E, *Fengzhengia mamingae* O'Flynn et al., 2022. F, *Isoxys acutangulus* Walcott, 1908 based on Legg and Vannier 2013. Scale bar represents 1 cm.

Indeterminate hour-glass shaped sternites are situated medially, in thoracic segments one–four (these are particularly evident in the phosphorous map; Figure 1G). A ventral plate-like structure is also associated with cephalic segments three–five (Figure 1C).

The terminal end of the body is visible in association with the tailpiece. It is narrow (13.8 mm in contrast to the tail, which is 55 mm wide) and lozenge-shaped (Figure 2G).

Remarks. In terms of preservation, *Oura megale* n. gen. n. sp. is dorsoventrally compressed, lies parallel to lamination and is well-articulated. This state of preservation suggests limited post-mortem transportation (Shu et al., 1999). Compactional folds in the tailpiece suggest localized, weak sclerotization. The animal may have suffered little damage due to post-mortem transportation but importantly, preparation of the specimen has definitely led to damage and consequent loss of characters. Neither post-FA head nor thoracic endopods remain. Even the sternites appear to have been damaged and so *O. megale* n. gen. n. sp. bears a superficial resemblance to radiodonts. Be this an artefact of preparation or taphonomy, certain characters are unobservable and affect the phylogenetic assessment of *O. megale* n. gen. n. sp. (discussed in a following section of this article; see also Sansom, 2016 in which preservation and phylogeny are discussed).

The multi-segmented head of *Oura megale* n. gen. n. sp., what little evidence remains of a head shield, and arthrodization betray its affiliation with Deuteropoda. *Oura megale* n. gen. n. sp. also possesses an anterior sclerite as do many other deuteropods, for example, the recently described *Kylinxia zhangi* Zeng, Zhao and Huang in Zeng et al., 2020, *Fengzhengia mamingae* O'Flynn et al., 2022, and artiopods [e.g., *Kuamaia lata* Hou, 1987 (see O'Flynn et al., 2024a)]. Furthermore, *O. megale* n. gen. n. sp. has lamellate exopods that resemble those of the deuteropod *Bushizheia yangi* O'Flynn and Liu in O'Flynn et al., 2020 (see O'Flynn et al., 2020, figure 1; 2024b, figure 2).

Oura megale n. gen. n. sp. exhibits especially long stalked eyes, a symplesiomorphy of Deuteropoda with a superficial resemblance to those of radiodonts, but also of some deuteropods (e.g., *Fengzhengia mamingae*) and so this character is not particularly useful phylogenetically. The head shield, which may have covered the eye stalks more completely in life, has almost entirely been excavated away.

Only three podomeres of the FA (the right one, specifically A1 in Figures 1 and 2) are preserved but they are certainly robust, each virtually as wide at the base as its associated podomere is long, and each endite is as long as its podomere is long. In this, *Oura megale* n. gen. n. sp. has much in common with the endites on the FAs of *Kylinxia zhangi*, the earliest branching deuteropod (see O'Flynn et al., 2023). It is uncertain whether there is one endite per podomere, or two.

Note that the plate, associated with cephalic segments three–five, could represent the hypostome (Figure 1), a deuteropodan synapomorphy (Ortega-Hernández, 2016). Hypostomes can extend backwards, the most extreme example being the Ordovician trilobite *Hypodicranotus striatulus* (Walcott, 1875) (see also Shiino et al., 2012, figure 1C–D). However, we are reluctant to assert this interpretation for this structure based on this single, poorly preserved specimen.

The division of the thorax into an anterior series of longer tergites (t1–10) and a posterior series of shorter ones (t11–15, see Figure 1A–E), that is, differentiation of tagmata, is more commonly seen in recent euarthropods. However, fuxianhuiids show this (Hou and Bergström, 1997), as does *Fengzhengia mamingae*, one of the earliest branching deuteropods (O'Flynn et al., 2022). Like *F. mamingae, Oura megale* n. gen. n. sp. has long and then short sternites, antero-posteriorly, the borders of which are perhaps most well-defined in the F1 map. But unlike *F. mamingae* and fuxianhuiids, no differentiation of tagmata is seen in terms of width.

This animal's tailpiece is clearly broad, and delta-shaped (Figure 2G). It is unlike the three paired tail flaps exhibited by anomalocaridids, *Opabinia* Budd, 1998 and isoxyids (Zeng et al., 2020, character 142; see their supplementary information). Nor are there three lobes to the tailpiece, as is the case in *Kylinxia zhangi*, where those three lobes are attached to the pygidium, which *Oura megale* n. gen. n. sp. does not have (cf. Zeng et al., 2020). Instead, the tailpiece of *O. megale* bears a greater resemblance to that of *Fengzhengia mamingae*, as interpreted in O'Flynn et al., (2022, figure 9), which is also somewhat delta-like (albeit backward-swept). It is important to mention, however, that neither tailpiece is well-preserved. *Fengzhengia mamingae,* like *K. zhangi,* also has a pygidium, which is not present in *O. megale* n. gen. n. sp.

Tuzoia Resser, 1929 (see Izquierdo-López and Caron, 2022), a bivalved arthropod from the

Burgess Shale, has been reconstructed with a tail conducive to swimming, a condition inferred in *F. mamingae* as in *Oura megale* n. gen. n. sp., but with two pairs of caudal rami (Izquierdo-López and Caron, 2022, figure 6–7). Furthermore, the tailpiece of *O. megale* n. gen. n. sp. appears to lack the terminal segment in *Tuzoia* (see Izquierdo-López and Caron, 2022, figure 6) and is less semicircular and more sub-triangular.

DISCUSSION

Phylogeny

Maximum parsimony analyses (Figures 4–5) and Bayesian analysis (Figure 6) recover *Oura*

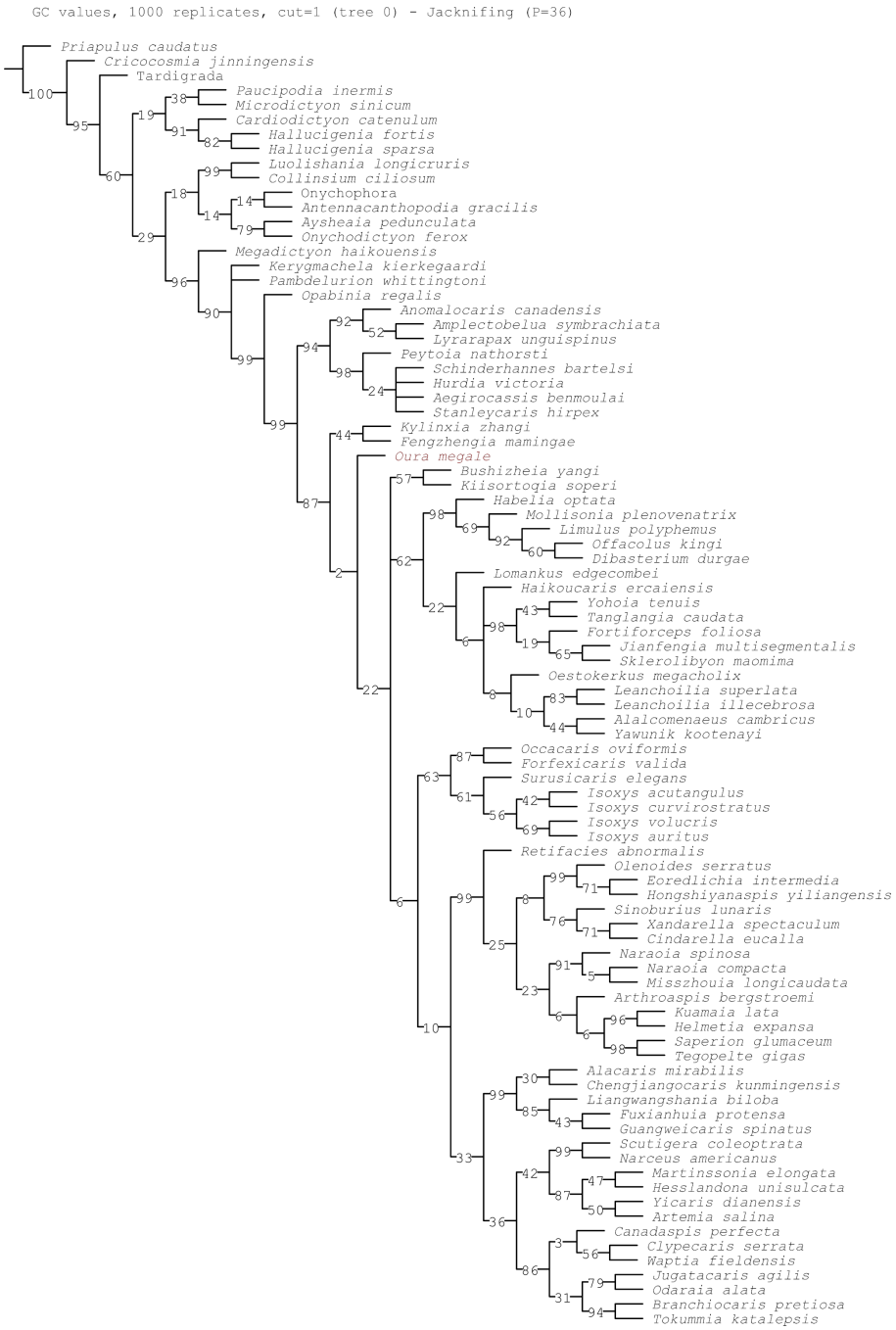

FIGURE 4. Consensus tree from phylogenetic analysis of panarthropod relationships based on a matrix of 283 characters and 88 taxa. Strict consensus of 368 most parsimonious trees with a score of 758 (consistency index = 0.45; retention index = 0.85) from analysis using equal weighting.

megale n. gen. n. sp. as a transitional form, bridging the morphological gap between the earliest branching deuteropods (*Kylinxia zhangi* and *Fengzhengia mamingae*) and the rest of Deuteropoda. Our phylogenetic topology provides a sequence of character evolution resulting in the loss of 'frontalmost appendages, shaft endite' also known from Radiodonta and *K. zhangi* (i.e., character 189; see Zeng et al., 2020), a node crownward of *O. megale.*

It is evident that over-preparation of the specimen has removed several key characters, including the left-side FA, the distal part of the right-side FA, the appendages on head segments three–five,

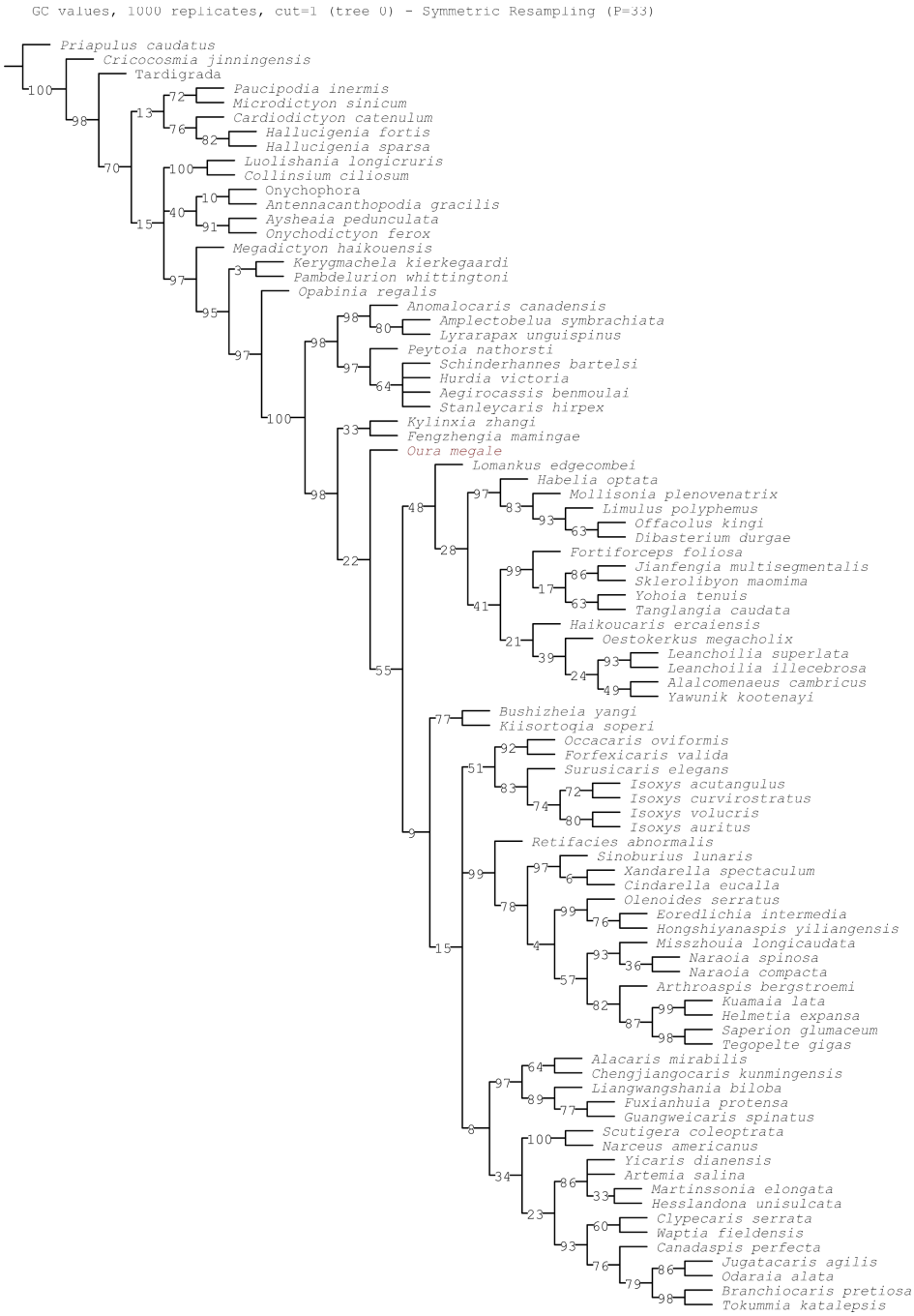

FIGURE 5. Consensus tree from phylogenetic analysis of panarthropod relationships based on a matrix of 283 characters and 88 taxa. Strict consensus of 3 most parsimonious trees with a score of 59.56497 (consistency index = 0.44; retention index = 0.84) from analysis using implied (concavity constant k = 3) weighting.

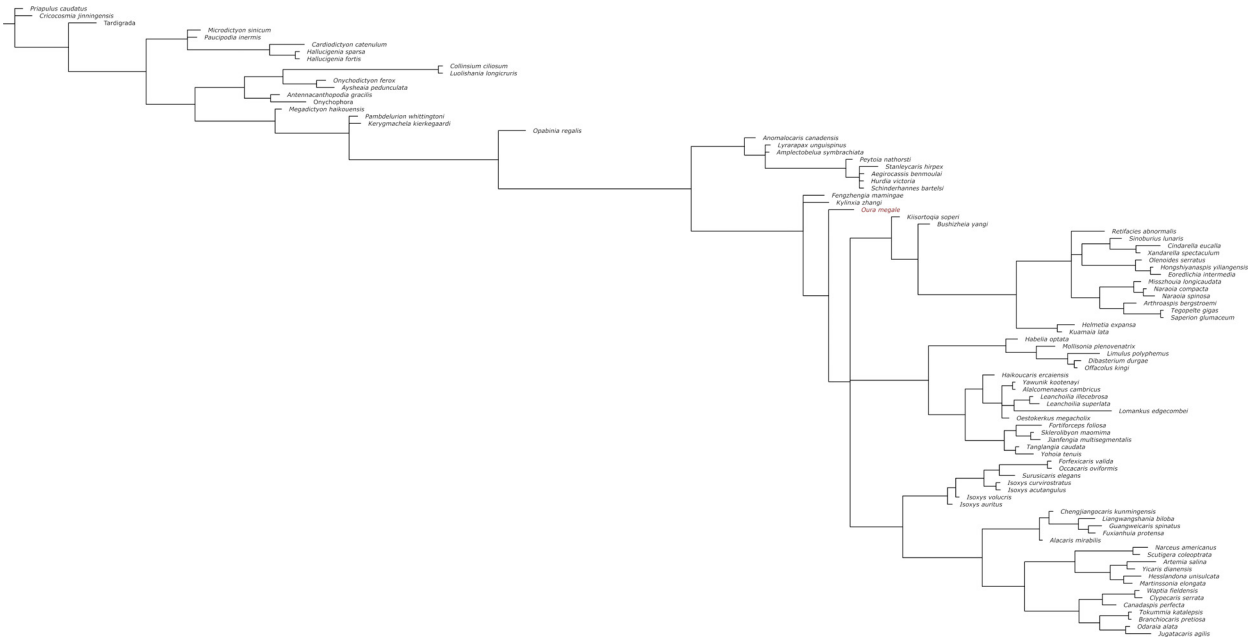

FIGURE 6. Consensus tree from phylogenetic analysis of panarthropod relationships based on a matrix of 283 characters and 88 taxa. 50% majority-rule consensus tree from a Bayesian analysis. The figure can be downloaded from the website https://palaeo-electronica.org/content/2025/5687-early-cambrian-deuteropod-oura-megale.

and the endopods on head segment six and thoracic segments (t1–15). Until more specimens of this unique euarthropod are recovered, any morphological interpretation should be tentative; uncertainty in the interpretation of head segmentation, for example, must not be overlooked, to which O'Flynn et al. (2024b) alluded (references therein). However, a six-segmented head organization [as in *K. zhangi* and extant mandibulates (Fusco and Minelli, 2013)] represents an ancestral situation for deuteropods (O'Flynn et al., 2023; see also O'Flynn et al., 2024a, b) and was already acquired by a common ancestor with the earliest branching deuteropod (i.e., *K. zhangi).* Under the scenario that *Oura megale* n. gen. n. sp. does indeed have a six-segmented head, phylogenetic analysis bolsters our confidence that the six-segmented head of living mandibulates is a deeply rooted, and conserved feature.

Palaeoecology

The interpretation of the swimming efficiency and manoeuvrability of *Oura megale* n. gen. n. sp. must rest on inferences from the morphology of its delta-shaped tailpiece and comparison with other taxa (Figure 3). O'Flynn et al. (2022) suggested that *Fengzhengia mamingae*, which has a cropped, backward-swept tailpiece, may have been an efficient swimmer, with reference to the hydrodynamic analysis of *Anomalocaris canadensis* Whiteaves, 1892. Sheppard et al. (2018, figure 3) demonstrated that the delta-shaped tailpiece (see also Figure 3A) of *A. canadensis,* enabled the radiodont to change direction rapidly, while its lateral lobes allowed for propulsion. By analogy, *O. megale* n. gen. n. sp. may have used its ogival delta tailpiece (Figure 3B) and exopods similarly to *A. canadensis,* as well as *F. mamingae* (Figure 3E).

The flow over a delta wing [e.g., in avian tails (Maybury et al., 2001) and extinct reptiles (Dyke et al., 2006)] is 'characterized by a pair of counter-rotating leading-edge vortices' (Botella et al., 2024, p. 1), that is, LEVs. LEVs, a source of lift, are also exploited by insects (e.g., Srygley, 2002) and bats (e.g., Johansson et al., 2016), and by aquatic animals (ostracoderms; Botella et al., 2024 and references therein). A delta-shape configuration (i.e., swept back with a triangular form reminiscent of the tailpiece of *Anomalocaris canadensis*), with its low aspect ratio, is conducive to speed and manoeuvrability (Li et al., 2022), but suffers from drag at low speeds (Mohamed et al., 2022 and references therein). An ovigal-shape configuration (i.e., the tailpiece of *Oura megale* n. gen. n. sp.), a variation of the delta, suffers from slightly less drag at lower speeds, but from slightly more drag at higher speeds (Bravo-Mosquera et al., 2018). We suggest that *A. canadensis* and the similarly sized

O. megale n. gen. n. sp. (see Figure 3A–B for context), may both have been capable nektonic predators, with *A. canadensis,* possibly, being somewhat more specialized for high-speed pursuit (Bicknell et al., 2023).

The tails of *Anomalocaris canadensis* and *Oura megale* n. gen. n. sp. further differ in that *A. canadensis* has a multi-vane geometry (Figure 3A–B), hence the three chevron shapes constructed in the hydrodynamic analysis of Sheppard et al., (2018). However, investigation of the two models (chevron and triangular) 'showed little difference', 'although the triangular model showed a small improvement in lift generation over the chevron model' (Sheppard et al., 2018, p. 710).

In *Oura megale* n. gen. n. sp., the posterior-most five thoracic segments are reduced, that is, they are shorter in comparison with those more anterior, and the fifteenth segment articulates with the tailpiece (Figures 1A–E, 2G). This differentiation of tagmata resembles that seen in *Fengzhengia mamingae* and could be an adaptation, in both euarthropods, for swimming, whereby a differentiated unit of tagmata bears a direct relationship to the tailpiece. That is to say, flexibility of the body in that portion is often used for swimming and, in particular steering, as seen in the tails of otters (Shiino et al., 2012 and references therein). But the effect on steering and/or propulsion of the tailpiece [as in many species of fish to which Sheppard et al. (2018) alluded] would require further studies. Nevertheless, the shape is of benefit to manoeuvres, that is, rapid change of direction.

The rapid manoeuvre-enabling, delta-shaped tailpiece, large, stalked eyes and probable paired raptorial frontal appendages of *O. megale* n. gen, n. sp. imply a predatory life habit in a nektonic or nekton-benthonic animal, as does its large size, comparable to that of large radiodonts, apex predators of the day. Fu et al. (2011a, b) and Paterson et al. (2010) discussed some of the aforementioned characters and their predatory implications in certain other early euarthropods, that is, isoxyids and radiodonts, respectively. In particular, 'strong locomotion' and its association with predation, is mentioned (Fu et al., 2011b, p. 850).

CONCLUSIONS

The body of *Oura megale* n. gen. n. sp., an especially large deuteropod (which rivals radiodonts in size), is fully arthrodized and so it consequently rests comfortably within Euarthropoda (e.g., Aria, 2019). It may have possessed raptorial FAs, of which the three proximal-most podomeres of the right-side FA are preserved. It also has large paddle-shaped exopods and a delta-shaped tailpiece, which may have contributed to high positional manoeuvrability.

The results of phylogenetic analyses, albeit hampered by the removal of key characters by over-preparation, resolves *Oura megale* n. gen. n. sp. as an early-branching deuteropod, bridging between the earliest-branching *Kylinxia zhangi* and *Fengzhengia mamingae* and all other deuteropods. Better material of this euarthropod will undoubtedly contribute to a more complete understanding of its phylogenetic relationships within Deuteropoda.

ACKNOWLEDGEMENTS

We thank an anonymous fossil collector for discovering, preparing and donating the specimen to the Yunnan Key Laboratory for Palaeobiology. We also thank M. Yu (Yunnan University) for assistance with photography. R. Melzer (Bavarian State Collection of Zoology, Munich) and H.-J. Mai (Yunnan University) are acknowledged for organizing the CT scans of the specimen, and we acknowledge the Advanced Microanalysis facility in the School of Archaeology and Ancient History (University of Leicester) for access to their Bruker M4 Tornado. We are indebted to the editors and two anonymous reviewers for their helpful comments. This study is supported by the Natural Science Foundation of Yunnan Province (grant number: 202401BC070012). Y. Liu is supported by the Yunnan Revitalization Talent Support Program and currently an Honorary Visiting Professor at the University of Leicester, supported by the Chinese Scholarship Council.

REFERENCES

Aria, C. 2019. Reviewing the bases for a nomenclatural uniformization of the highest taxonomic levels in arthropods. Geological Magazine, 156:1463–1468. https://doi.org/10.1017/S0016756819000475

Beckhoff, B., Kanngießer, B., Langhoff, N., Wedell, R., and Wolf, H. 2006. Handbook of Practical X-Ray Fluorescence Analysis, First Edition. Springer Berlin, Heidelberg. https://doi.org/10.1007/978-3-540-36722-2

Bengtson, S. 2000. Teasing fossils out of shales with cameras and computers. Palaeontologia Electronica, 3.1.4A:1–14. https://palaeo-electronica.org/2000_1/fossils/issue1_00.htm

Bergström, J. and Hou, X.-G. 1998. Chengjiang arthropod and their bearing on early arthropod evolution. In Edgecombe, G.D. (ed.), Arthropod Fossils and Phylogeny. Columbia University Press, New York.

Bicknell, R.D.C., Schmidt, M., Rahman, I.A., Edgecombe, G.D.E., Gutarra, S., Daley, A.C., Melzer, R.R., Wroe, S., and Paterson, J.R. 2023. Raptorial appendages of the Cambrian apex predator *Anomalocaris canadensis* are built for soft prey and speed. Proceedings of the Royal Society B, 290:20230638.

Botella, H., Fariña, R.A., and Huera-Huarte, F. 2003. Delta wing design in earliest nektonic vertebrates. Communications Biology, 7:1153. https://doi.org/10.1038/s42003-024-06837-8

Bravo-Mosquera, P.D., Abdalla, A.M., and Catalano, F.M. 2018. Evaluation of delta wing effects on stealth-aerodynamic features for non-conventional fighter aircraft. 31st Congress of the International Council of the Aeronautical Sciences, Belo Horizonte, Brazil.

Briggs, D.E.G. and Parry, L.A. 2022. Putting heads together. Science, 378:831–832. https://doi.org/10.1126/science.add7372

Budd, G.E. 1998. Stem-group arthropods from the lower Cambrian Sirius Passet fauna of north Greenland. In the Systematics Association Special Volume Series: Fortey, R.A. and Thomas, R.H. (eds.), Arthropod Relationships 55. Springer, Dordrecht. https://doi.org/10.1007/978-94-011-4904-4_11

Budd, G.E. 2021. The origin and evolution of the euarthropod labrum. Arthropod Structure & Development, 62:101048. https://doi.org/10.1016/j.asd.2021.101048

Chipman, A. 2024. The development and evolution of arthropod tagmata. Proceedings of the Royal Society B, 292:20242950. https://doi.org/10.1098/repb.2024.2950

Daley, A. and Edgecombe, G.D. 2014. Morphology of *Anomalocaris canadensis* from the Burgess Shale. Journal of Paleontology, 88:68–91. https://doi.org/10.1666/13-067

Dyke, G.J., Nudds, R.L., and Rayner, J.M.V. 2006. Flight of *Sharovipteryx mirabilis*: the world's first delta-winged glider. Journal of Evolutionary Biology, 19:1040–1043. https://doi.org/10.1111/j.1420-9101.2006.01105.x

Edgecombe, G.D., García-Bellido, D.C., and Paterson, J.R. 2011. A new leanchoiliid megacheiran arthropod from the lower Cambrian Emu Bale Shale, south Australia. Acta Palaeontologica, 56:385–400.

Friedrich, M. 2003. Evolution of insect eye development: first insights from fruit fly, grasshopped and flour beetle. Integrative and Comparative Biology, 43:508–21. https://doi.org/10.1093/icb/43.4.508

Fu, D.-J., Zhang, X.-L., and Shu, D.-G. 2011a. A venomous arthropod in the early Cambrian sea. Chinese Science Bulletin, 56:1532–1534. https://doi.org/10.1007/s11434-011-4371-6

Fu, D.-J., Zhang, X.-L., and Shu D.-G. 2011b. Soft anatomy of the early Cambrian arthropod *Isoxys curvirostratus* from the Chengjiang biota of south China with a discussion on the origination of great appendages. Acta Paleontologica Polonica, 56:843–852.

Fusco, G. and Minelli, A. 2013. Arthropod segmentation and tagmosis, p. 197–221. In Minelli, A., Boxshall, G., and Fusco, G. (eds.), Arthropod Biology and Evolution. Springer. https://doi.org/10.1007/978-3-642-36160-9_9

Gabbott, S.E., Hou, X.-G., Norry, M.J., and Siveter, D.J. 2004. Preservation of early Cambrian animals of the Chengjiang biota. Geology, 32:901–904. https://doi.org/10.1130/G20640.1

Goloboff, P.A. and Catalano, S.A. 2016. TNT, version 1.5, with a full implementation of phylogenetic morphometrics. Cladistics, 32:221-238. https://doi.org/10.1111/cla.12160

Gueriau, P. 2018. Show me your yttrium, and I will tell you who you are: implications for fossil imaging. Palaeontology, 61:981–990. https://doi.org/10.1111/pala.12377

Hou, X.-G. 1987. Three new large arthropods from the lower Cambrian, Chengjiang, eastern Yunnan. Acta Palaeontologica Sinica, 26:272–285.

Hou, X.-G., Bergström, J. 1997. Arthropods of the lower Cambrian Chengjiang fauna, south-west China. Fossils & Strata, 45:1–117. https://doi.org/10.18261/8200376931-1997-01

Hou, X.-G., Siveter, D.J., Siveter, D.J., Aldridge, R.J., Cong, P.-Y., Gabbott, S.E., Ma, X.-Y., Purnell, M.A., and Williams, M. 2017. The Cambrian Fossils of Chengjiang, China: The Flowering of Early Animal Life, Second Edition. John Wiley & Sons.

Izquierdo-López, A. and Caron, J.-B. 2022. The problematic Cambrian arthropod *Tuzoia* and the origin of mandibulates revisited. Royal Society Open Science, 9:220933. https://doi.org/10.1098/rsos.220933

Kimmig, J. and Schiffbauer, J.D. 2024. A modern definition of Fossil-Lagersätten. Trends in Ecology & Evolution, 39:621–624.

Lankester, R.E. 1904. The structure and classification of the Arthropoda. Quarterly Journal of Microscopical Science, 47:523–582. https://doi.org/10.1242/jcs.s2-47.188.523

Legg, D.A. and Vannier, J. 2013. The affinities of the cosmopolitan arthropod *Isoxys* and its implications for the origin of arthropods. Lethaia, 46:540–550. https://doi.org/10.1111/let.12032

Lei, X.-T., Cong, P.-Y., Zhang, S.-N., Wei, F., and Anderson, R.P. 2024. Unveiling an ignored taphonomic window in the early Cambrian Chengjiang biota. Geology, 52:753–758. https://doi.org/10.1130/G52215.1

Li, X., Feng, L.-H., and Wang, Q.-M. 2023. Wing rock mode and its mechanism of a flying-wing aircraft. Flow, 3:e38. https://doi.org/10.1017/flo.2023.30

Maybury, W.J., Rayner, J.M.V., and Couldrick, L.B. 2001. Lift generation by the avian tail. Proceedings of the Royal Society B, 268:1443–1448. https://doi.org/10.1098/rspb.2001.1666

Mohamed, M.A., Afgan, I., Salim, M.H., and Mohamed, I.K. 2022. Low speed aerodynamic characteristics of non-slender delta wing at low angles of attack. Alexandria Engineering Journal, 61:9427–9435. https://doi.org/10.1016/j.aej.2022.03.003

Nixon, K.C. 2002. WinClada ver. 1.00.08. Ithaca, New York, Renner and Weerasooriya, USA.

O'Flynn, R.J., Audo, D., Williams, M., Zhai, D.-Y., Chen, H., and Liu, Y. 2020. A new euarthropod with 'great appendage'-like frontal head limbs from the Chengjiang Lagerstätte, south-west China. Palaeontologia Electronica, 23(2):a36. https://doi.org/10.26879/1069

O'Flynn, R.J., Williams, M., Yu, M.-X., Harvey, T.H.P., and Liu, Y. 2022. A new euarthropod with large frontal appendages from the early Cambrian Chengjiang biota. Palaeontologia Electronica, 25(1):a6. https://doi.org/10.26879/1069

O'Flynn, R.J., Liu, Y., Hou, X.-G., Mai, H.-J., Yu, M.-X., Zhuang, S.-L., Williams, M., Guo, J., and Edgecombe, G.D. 2023. The early Cambrian *Kylinxia zhangi* and evolution of the arthropod head. Current Biology, 33:4006–4013. https://doi.org/10.1016/j.cub.2023.08.022

O'Flynn, R.J., Williams, M., Liu, Y., Hou, X.-G., Guo, J., and Edgecombe, G.D. 2024a. The early Cambrian *Kuamaia lata*, an artiopodan euarthropod with a raptorial frontal appendage. Journal of Paleontology, 98:808–820. https://doi.org/10.1017/jpa.2024.33

O'Flynn, R.J., Williams, M., Yu, M.-X., Guo, J., Audo, D., Schmidt, M., Mai, H-J., Liu, Y., and Edgecombe, G.D. 2024b. The early Cambrian *Bushizheia yangi* and head segmentation in upper stem-group euarthropods. Papers in Palaeontology, 10:e1556. https://doi.org/10.1002/spp2.1556

Ortega-Hernández, J. 2016. Making sense of 'lower' and 'upper' stem-group Euarthropoda, with comments on the strict use of the name Arthropoda von Siebold, 1848. Biological Reviews,

91:255–273.
https://doi.org/10.1111/brv.12168
Ortega-Hernández, J., Janssen, R., and Budd, G.E. 2017. Origin and evolution of the panarthropod head — a palaeobiological and developmental perspective. Arthropod Structure & Development, 46:354–379.
https://doi.org/10.1016/j.asd.2016.10.011
Parry, L.A., Briggs, D.E., Ran, R.-X., O'Flynn, R.J., Mai, H.-J., Clark, E.G., and Liu, Y. 2024. A pyritized Ordovician leanchoiliid arthropod. Current Biology, 34:1–9.
https://doi.org/10.1016/j.cub.2024.10.013
Paterson, J.R., Edgecombe, G.D., and García-Bellido, D.C. 2010. Disparate compound eyes of Cambrian radiodonts reveal their developmental growth mode and diverse visual ecology. Science Advances, 6:eabc6721.
https://doi.org/10.1126/sciadv.abc6721
Resser, C.E. 1929. New lower and middle Cambrian Crustacea. Proceedings of the United States National Museum, 76:1–18.
Ronquist, F., Teslenko, M., van der Mark, P., Ayres, D.L., Darling, A., Höhna, S., Larget, B., Liu, L., Suchard, M.A., and Huelsenbeck, J.P. 2012. MrBayes 3.2: efficient Bayesian phylogenetic inference and model choice across a large model space. Systematic Biology, 61:539–542.
https://doi.org/10.1093/sysbio/sys029
Sansom, R. 2016. Preservation and phylogeny of Cambrian ecdysozoans tested by experimental decay of *Priapulus*. Scientific Reports, 6:32817.
https://doi.org/10.1038/srep32817
Sheppard, K.A., Rival, D.E., and Caron, J.-B. 2018. On the hydrodynamics of *Anomalocaris* tail fins. Integrative and Comparative Biology, 58:703–711.
https://doi.org/10.1093/icb/icy014
Shiino, Y., Kuwazura, O., Suzuki, Y., and Ono, S. 2012. Swimming capability of the remopleuridid trilobite *Hypodicranotus striatus*: hydrodynamic functions of the exoskeleton and the long, forked hypostome. Journal of Theoretical Biology, 300:293–8
Shu, D.-G., Vannier, J., Luo, H.-L., Chen, L., Zhang, X.-L., and Hu, S.-X. 1999. Anatomy and lifestyle of *Kunmingella* (Arthropoda, Bradoriida) from the Chengjiang fossil Lagerstätte (lower Cambrian; south-west China). Lethaia, 32:279–298.
Schneider, C.A., Rasband, W.S., and Eliceriri, K.W. 2012. NIH Image to ImageJ: 25 years of image analysis. Nature Methods, 9:671–675.
https://doi.org/10.1038/nmeth.2089
Vinther, J. 2022. Evolution: the arthropod brain — a saga in three parts. Current Biology, 32:833–836.
https://doi.org/10.1016/j.cub.2022.06.091
Walcott, C.D. 1875. New species of trilobite from the Trenton Limestone at Trenton Falls, New York. Cincinnati Quarterly Journal of Science, 2:347–349.
Walcott, C.D. 1908. Mount Stephen rocks and fossils. The Canadian Alpine Journal, 1:232–248.
Whiteaves, J.F. 1892. Description of a new genus and species of phyllocarid Crustacea from the middle Cambrian of Mount Stephen, B.C. Canadian Record of Science, 5:205–208.
Zeng, H., Zhao, F.-C., Niu, K.-C., Zhu, M.-Y., and Huang, D.-Y. 2020. An early Cambrian euarthropod with radiodont-like raptorial appendages. Nature, 588:101–105.
https://doi.org/10.1038/s41586-020-2883-7
Zhang, X.-L., Liu, Y., O'Flynn, R. J., Schmidt, M., Melzer, R. L., Hou, X.-G., Mai, H.-J., Guo, J., Yu, M.-X., and Ortega-Hernández, J. 2022. Ventral organization of *Jianfengia multisegmentalis* Hou, and its implications for the head segmentation of megacheirans. Palaeontology, 65:e12624.
https://doi.org/10.1111/pala.12624

APPENDIX 1.

Phylogenetic matrix is available for download at https://palaeo-electronica.org/content/2025/5687-early-cambrian-deuteropod-oura-megale.